INTERNATIONAL SOCIETY FOR
SOIL MECHANICS AND
GEOTECHNICAL ENGINEERING

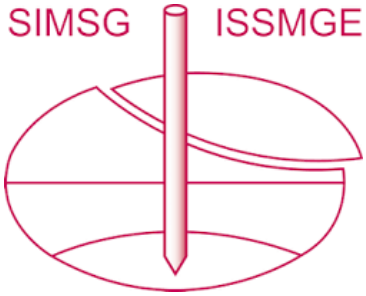

This paper was downloaded from the Online Library of the International Society for Soil Mechanics and Geotechnical Engineering (ISSMGE). The library is available here:

https://www.issmge.org/publications/online-library

This is an open-access database that archives thousands of papers published under the Auspices of the ISSMGE and maintained by the Innovation and Development Committee of ISSMGE.

Effect of Compaction Stresses on Performance of Back-to-Back Retaining Walls

Effet des contraintes de compactage sur la performance des murs de soutènement dos à dos

Umashankar Balunaini, Sasanka Mouli Sravanam, Madhira R Madhav
Associate Professor, Research student, Visiting Professor, Civil Engineering Department, IIT Hyderabad, India, buma@iith.ac.in

ABSTRACT: Back-to-back reinforced soil retaining walls are commonly used for approach embankments of bridges and flyovers. Existing design guidelines (FHWA/BS/IS codes) do not provide a mechanistic approach to design back-to-back reinforced soil retaining walls. Lateral pressures on the facing and at end of reinforced zone are required for stability checks (both internal and external). During stage-wise construction of back-to-back walls, compaction stresses should be incorporated to obtain realistic lateral earth pressures on the walls. The present paper describes the effect of the compaction stresses on the lateral pressures in such reinforced soil retaining walls. The variation of lateral pressures at the end of reinforced zone along the depth of the wall is obtained from numerical modeling of back-to-back reinforced soil walls. A surcharge load of 30 kPa is applied at the end of the construction of the wall. It is observed that the effect of surcharge load is not significant after certain depth of the wall for lower spacing between walls to wall height ratios. A comparison on lateral pressures with and without compaction stresses for different distances between the ends of reinforcements of two walls is presented. Effect of connection of reinforcement is also studied.

Résumé : L'une à la suite des murs de terre renforcée sont couramment utilisés pour les remblais d'approche des ponts et des survols. Lignes directrices existantes (FHWA/BS/EST codes) ne fournissent pas une approche mécaniste pour concevoir des murs de terre renforcée. Les pressions latérales sur la face et à la fin de la zone renforcés sont nécessaires pour les contrôles de stabilité (internes et externes). Lors de l'étape-sage construction de retour-à-dos, le tassement des murs souligne devraient être intégrés pour obtenir des pressions latérales réalistes sur les murs. Le présent document décrit l'effet de la compaction du stress sur le pressions latérales dans des murs de terre renforcée. La variation des pressions latérales à la fin de la zone renforcée le long de la profondeur du mur est obtenue à partir de la modélisation numérique des murs de terre renforcée. Un supplément de charge de 30 kPa est appliquée à la fin de la construction du mur. Il est observé que l'effet de la surcharge n'est pas significative après certaine profondeur du mur pour réduire l'espacement entre les murs à hauteur du mur de ratios. Une comparaison sur les pressions latérales avec et sans contraintes de compactage pour différentes distances entre les extrémités des renforts de deux murs est présenté. Effet de la liaison de renfort est également étudié.

KEYWORDS: Back-to-back walls, Compaction stresses, Surcharge loads, Lateral pressures, FLAC

1 INTRODUCTION

Compaction and surcharge induced lateral pressures are important in analysis and design of mechanically stabilized earth (MSE) retaining walls. Compaction induced lateral stresses in single reinforced retaining wall was well studied and reported in the literature (e.g. Duncan & Seed, 1986., Bathurst et al., 2009, Wu & Pham, 2010, and Mirmoradi & Ehrlich, 2015). The interaction between the two walls of back-to-back retaining walls will be significant if they are relatively close to one another.

Back-to-back MSE walls were analyzed using Finite Element and Finite Difference methods under working stress and limit state conditions (Han & Leshchinsky 2010, El-Sherbiny et al. 2013, Djabri & Benmebarek 2016). Studies were focused on the effects of wall spacing to height ratios on lateral pressures, tensile forces in reinforcement, and the formation of critical slip surfaces. Studies on the effects of compaction and surcharge loads in back-to-back MSE walls are limited in the literature. In the present study, the effect of compaction and surcharge stresses for various spacing to height ratios of back-to-back walls is analysed in working stress method.

2 PROBLEM STATEMENT

The main objective of the paper is to study the effect of compaction stresses and surcharge loads on lateral pressures in back-to-back walls using numerical model based on Finite Difference scheme. Parameteric study on effects of stiffness of reinforcement and wall spacing to height (*W/H)* ratios is carried out.

3 MODEL DESCRIPTION

The Finite difference program, Fast Lagrangian Analysis of Continua (FLAC), was used for the analysis (Itasca 2011). Back-to-back walls of height 6m was considered. Length of reinforcement was 4.2 m (0.7 times the height of the wall). The distance (gap) between the ends of the reinforcements extending from the two walls was varied from 0 to 0.6H so that W/H ratio ranges from 1.4 to 2.0. Vertical spacing between the reinforcement was taken as 0.6 m for the entire parametric study.

Mesh convergence was performed and the size of the grid was taken as approximately equal to 0.1m. Large-strain mode was activated so that the coordinates of the grid points were updated at every step. This ensures accuracy in the numerical model, especially when large strains were developed in the material.

The foundation soil was assumed to be rigid. Reinforced soil was simulated as homogenous, isotropic, elastic-perfectly plastic using Mohr-Coulomb failure criterion. Table 1 provides the properties of reinforced soil/backfill, foundation soil, and facing panel.

Deformation modulus of the soil is dependent on the confining stress (Duncan et al., 1980), and as such was updated at every stage using the procedure given in Hatami and Bathurst (2005). Equation given by Duncan et al. (1980) was used [Eq. (1)].

$$E_t = \left[1 - \frac{R_f(1-sin\phi)(\sigma_1-\sigma_3)}{2c.cos\phi+2\sigma_3.sin\phi}\right]^2 . K_e . P_{atm} . \left(\frac{\sigma_3}{P_{atm}}\right)^n \qquad (1)$$

where, E_t is the tangent elastic modulus, R_f is the failure ratio, K_e is the elastic modulus number, n is the elastic modulus exponent, P_{atm} is the atmospheric pressure, ϕ is the angle of shearing resistance of soil, c is the cohesion intercept of soil, σ_1 is the effective vertical pressure (overburden), and σ_3 is the effective lateral confining pressure.

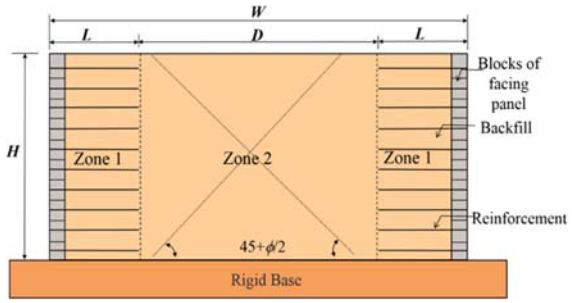

Figure 1. Schematic of back-to-back MSE walls

The wall facing was modelled as modular blocks of size 0.3 x 0.2m. Material properties of modular blocks were assumed to be equal to that of concrete material (Table 1).

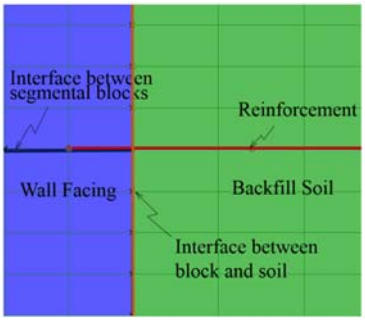

Figure 2. Mesh configuration and interfaces represented in FLAC

Table 1 Properties of the foundation soil, reinforced and retained backfills

Properties	Reinforced soil	Foundation soil	Modular blocks
Material type	Mohr-Coulomb	Mohr-Coulomb	Elastic
Cohesion (kPa)	0	1000	-
Angle of shearing resistance (ϕ) in deg.	34	35	-
Dilation angle in deg.	10	0	-
Shear Modulus (kPa)	3.846e4	3.846e4	8.70e6
Bulk Modulus (kPa)	8.333e4	8.332e4	9.52e6
Density (kg/m^3)	1800	1800	2400

Table 2 Constants used in the equation for stress dependent modulus of backfill soil

Properties	Reinforced soil
Elastic modulus number (K_e)	1150
Bulk modulus number (K_b)	575
Elastic modulus exponent (n)	0.5
Bulk modulus exponent (m)	0.5
Failure ratio (R_f)	0.86

Table 3 Reinforcement properties

Properties	Cable element
Stiffness (J) (kN/m)	500, 50000
Poisson's ratio (υ)	0.3

Reinforcement was simulated as cable element. Cable element in FLAC is a two-noded, one-dimensional element with high tensile stiffness and negligible compressive stiffness. Reinforcement was assumed to be rigidly fixed at the one end of the cable element to nodes of the wall facing to simulate the rigid connection that exists in the field. Table 3 provides the reinforcement properties. The reinforcement stiffness of 500 kN/m and 50000 kN/m were considered in the study representing extensible and inextensible reinforcements. Reinforcements of the two walls were connected in the middle in one of the cases (which was denoted as "connected" case hereafter) .

The numerical model considered the stage-wise construction of back-to-back walls. Compaction stresses were applied at every stage over the surface of soil layer. Each lift of 0.3m height of soil was first placed. Subsequently, a static vertical stress of 8 kPa was applied to simulate the compaction stresses (Hatami and Bathurst 2005) and the model was solved for equilibrium. The deformation modulus was then updated using Eq. (1) (using the constants mentioned in Table 2), and again solved for equilibrium. The applied vertical stress was then removed, and again the modulus was updated and solved. The next layer of soil was now placed on the deformed grid of the previous layer. At every stage, the maximum unbalanced force ratio was maintained to be less than 1e-3. Surcharge load of 30 kPa was applied on the surface of the wall at the end of construction of the entire wall.

4 RESULTS

Normalized lateral pressures at the end of reinforcement were plotted for three cases: **Case (a)** without compaction stresses and surcharge, **Case (b)** with compaction stresses and no surcharge load, and **Case (c)** with compaction stresses and surcharge load.The lateral pressures were normalized with the product of unit weight and total height of the wall ($\gamma * H$) and the depth was normalized with respect to the height of the wall [Eq. (2), Eq. (3) and Eq. (4)]. Linear trend lines were found to provide a good fit for the variation of lateral earth pressures with depth (regression coefficient, $R^2 \approx 1.0$).

The variation of lateral earth pressure at the end of the reinforced zone showed a bilinear variation with the slope increasing sharply beyond a certain depth. Accordingly, a term *critical depth*, Z_c, was defined as the depth at which the coefficient of lateral pressure (K) changes with respect to the depth of the wall. It may be noted that the inverse of the slope of lateral pressure profiles indicate the coefficient of the lateral pressure (K).

$$\sigma_{hr}{}^{*} = \frac{\sigma_{hr}}{\gamma H} \quad (2)$$

$$\sigma_{hf}{}^{*} = \frac{\sigma_{hf}}{\gamma H} \quad (3)$$

$$Z^{*} = \frac{Z}{H} \quad (4)$$

4.1 W/H=1.40

Figure 3 shows the lateral pressures at the end of reinforcement zone for the case of W/H=1.4 and J= 500 kN/m. The lateral pressures were much less than the active condition for the three cases considered. The reduction of lateral stresses below active condition near end of reinforcement may be attributed to the relative settlement between reinforced and unreinforced zones, shown as *Zone 1* and *Zone 2* in Figure 1, leading to arching effect. The proposed arching phenomenon is similar to that of flow of granular material in silos leading to reduction in vertical stresses (Widisinghe and Sivakugan 2012). This was found to be significant for low W/H ratios.

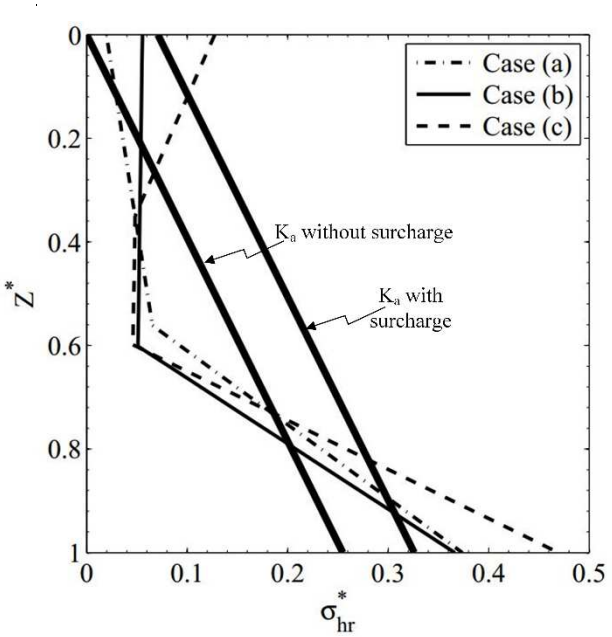

Figure 3. Lateral pressures at the end of reinforced zone for *W/H*=1.4 with *J*=500 kN/m

It was observed that beyond certain depth, the lateral stresses under compaction stresses showed lower values compared to those without compaction stresses [Case (a) and Case (b)]. This could be due to arching effect being predominant at the end of reinforcement for the compacted case. The lateral pressures due to compaction stresses and surcharge loads follow a trilinear pattern [Case (c)] with higher values near the top than for Case (b) and the values coinciding with those for with compaction stresses below depths of *0.3H*, indicating that the increment in the lateral pressures due to surcharge is almost negligible below this depth of the wall. This implies that surcharge induced lateral stresses decrease with depth.

Figure 4 shows the variation of lateral pressures at the end of reinforcement zone with depth for the case with *W/H*=1.40, and *J*= 50000 kN/m. The critical depths Z_c in this case were higher than that of *J*=500 kN/m case. Z_c values increased from 0.6*H* to about 0.8*H*. The value of Z_c remains almost constant for all loading conditions for a particular *W/H* ratio and reinforcement stiffness value.

The lateral pressures due to surcharge load and compaction stresses showed bilinear variation for this case. The effect of surcharge load extended to higher depths for reinforcement with high stiffness (*J*=50000 kN/m) than that for reinforcement with low stiffness (*J*=500 kN/m). The higher reinforcement stiffness might have led to extending the influence depth of surcharge induced lateral pressures.

4.2 W/H=2.0

Figure 4 shows the variation of lateral pressures at the end of reinforcement zone with depth for the case of *W/H*=2.0 and *J*=500 kN/m. In this case, the back-to-back walls behaved independently. The lateral pressures were close to active condition under no compaction stresses [Case (a)]. The increase in the lateral pressures at the bottom of the wall was due to the rigid boundary condition of the foundation soil. The variation depends on stiffness of foundation soil (Huang et al. 2010). When compaction stresses were applied, the lateral pressures were higher near the top and slightly lower at the bottom of the wall for Case (b) in comparison to Case (a).

The increase in lateral pressures due to surcharge load and compaction stresses extended near to the bottom of the wall for both reinforcement stiffness values, *J*=500 kN/m and *J*=50000 kN/m. However with *J*=500 kN/m, the effect of compaction stresses was nullified and lateral pressures were nearly equal to $K^*(\gamma^*H+q)$ (K_a with surcharge) up to depth equal to 0.7*H*.

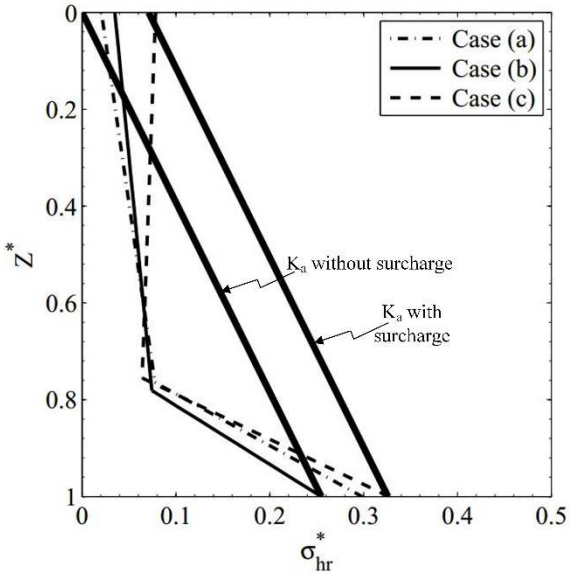

Figure 4. Lateral pressures at the end of reinforced zone for *W/H*=1.4 with *J*=50000 kN/m

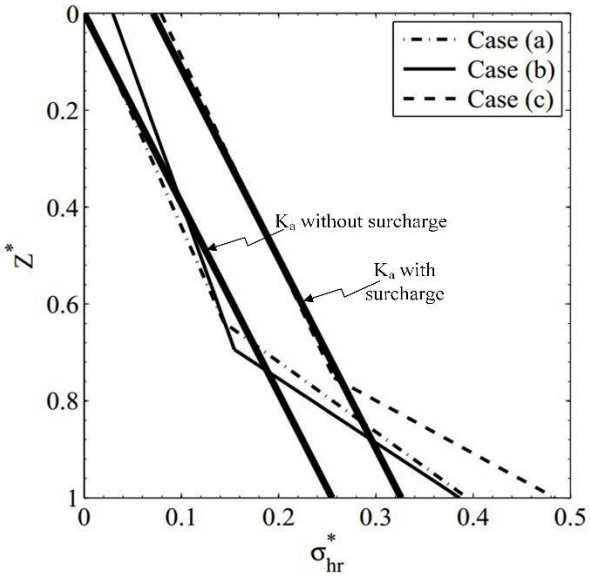

Figure 5. Lateral pressures at the end of reinforced zone for *W/H*=2.0 with *J*=500 kN/m

4.3 W/H=1.40 Connected case

Normalized lateral pressures at the facing were plotted for the connected and unconnected cases corresponding to reinforcement stiffness, *J*, equal to 50000 kN/m (Figure 7). The lateral pressures at the facing for unconnected case were almost equal to those of active earth pressures for Case (c). In case (b), the lateral pressures at the facing were higher and parallel to K_a line with surcharge, shown in Figure 7, denoting the effect of compaction stresses leading to higher lateral pressures. For connected reinforcement, the lateral pressures were found to be less than those corresponding to active condition. The vertical pressures were also found to be less than the overburden

stresses indicating that arching effect was significant for the connected reinforcements. The effect of surcharge induced lateral pressures was found to be minimal beyond a depth of 0.8*H* from top of the wall.

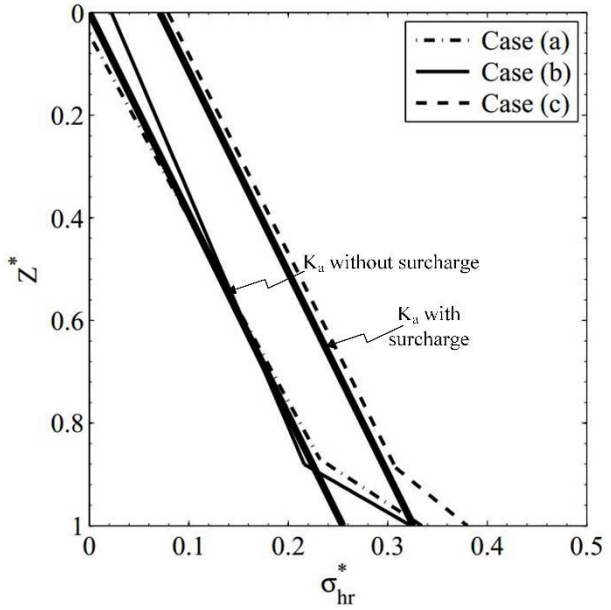

Figure 6. Lateral pressures at the end of reinforced zone for *W/H*=2.0 with *J*=50000 kN/m

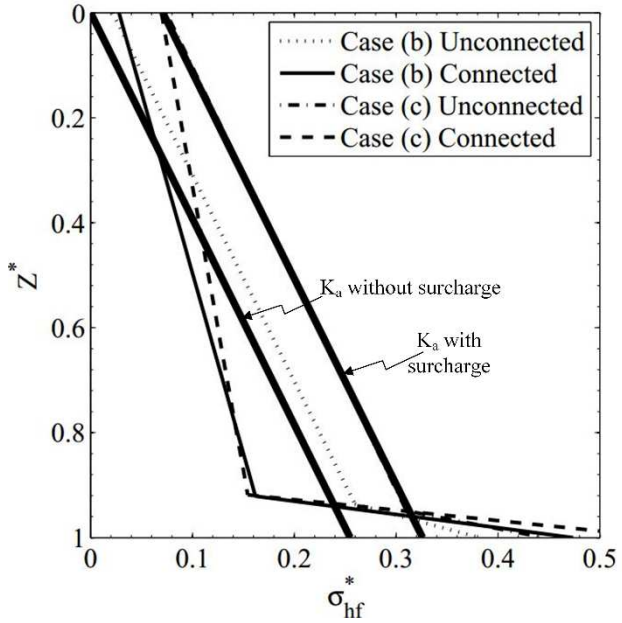

Figure 7. Comparison between connected and unconnected cases for lateral pressures at the facing and *J*=50000 kN/m

5 CONCLUSIONS

Normalized lateral pressures of back-to-back walls were plotted against the height of the wall for the cases of *W/H*=1.4 and 2.0 with reinforcement stiffness equal to *J*=500 and 50000 kN/m. The following conclusions can be drawn from the study:

1. The lateral pressures at the end of reinforcement are bilinear for almost both the *W/H* ratios. It is much less than the active earth pressures for *W/H* =1.40.
2. As the reinforcement stiffness increases, the value of Z_c increases. Value of Z_c increases even with increase in *W/H* ratio. However, it remains almost constant for different loading conditions.
3. When the reinforcement stiffness and *W/H* ratio are low, surcharge induced lateral pressures decreases much faster with depth than that for the condition with high *W/H* ratio and reinforcement stiffness. For example, surcharge induced lateral pressures in *W/H*=1.4 and *J*=500 kN/m coincided with no surcharge load case at about 0.35*H*. While for *W/H*=2.0 and *J*=50000 kN/m, the effect of both surcharge and compaction stress extended till the bottom of the wall.
4. In the lower half of the wall, the lateral pressures in the compacted cases are slightly less than those of the without compaction cases.
5. Surcharge and compaction induced lateral pressures at the facing extend till bottom of the wall in the unconnected reinforcement of high stiffness. However, for connected case, the effect reduces with depth of the wall due to arching phenomenon.

6 REFERENCES

Bathurst, R.J., Nernheim A., Walters D.L., Allen, T.M., Burgess, P. and Saunders, D.D. 2009. Influence of reinforcement stiffness and compaction on the performance of four geosynthetic-reinforced soil walls. *Geosynthetics International* 16 (1) 43–59.

Djabri M. and Benmebarek S. 2016. FEM analysis of back-to-back geosynthetic-reinforced soil retaining walls. *International Journal of Geosynthetics and Ground Engineering* 2 (3), 26.

Duncan J.M., Byrne P., Wong K.S. and Mabry P. 1980. Strength, stress–strain and bulk modulus parameters for finite element analysis of stresses and movements in soil masses. *Department of Civil Engineering, University of California*, Berkeley, California, USA, Report No. UCB/GT/80-01.

Duncan J. M. and Seed R.B. 1986. Compaction- induced earth pressures under K_o-conditions. *Journal of geotechnical engineering* 112 (1), 23–43.

El-Sherbiny R., Ibrahim, E. and Salem, A. 2013. Stability of back-to-back mechanically stabilized earth walls. In *Geo-Congress*, San Diego, California, USA, 555–565.

Han J. and Leshchinsky, D. 2010. Analysis of back-to-back mechanically stabilized earth walls. *Geotextiles and Geomembranes* 28 (3), 262–267.

Hatami K. and Bathurst R.J. 2005. Development and verification of a numerical model for the analysis of geosynthetic-reinforced soil segmental walls under working stress conditions. *Canadian Geotechnical Journal* 42 (4), 1066–1085.

Huang B., Bathurst R.J., Hatami K. and Allen T.M. 2010. Influence of toe restraint on reinforced soil segmental walls. *Canadian Geotechnical Journal* 47 (8), 885–904.

Itasca. 2011. FLAC-Fast Langragian Analysis of Continua Version 7.00. *Itasca Consulting Group Inc., Minneapolis.*

Mirmoradi S.H. and Ehrlich M. 2015. Modeling of the compaction-induced stress on reinforced soil walls *Geotextiles and Geomembranes* 43 (1), 82–88.

Widisinghe S. and Sivakugan N. 2012. Vertical stresses within granular materials in silos. *ANZ Conference Proceedings 590* (61), 590–595.

Wu J. and Pham T. 2010. An analytical model for evaluation of compaction-induced stresses in a reinforced soil mass. *International Journal of Geotechnical Engineering* 4 (4), 549–556.